Desalination and Water Treatment
www.deswater.com

17 (2010) 248–254
May

1944-3994/1944-3986 © 2010 Desalination Publications. All rights reserved
doi: 10.5004/dwt.2010.1725

Organic fouling behavior of anion exchange membranes prepared from chloromethyl styrene and divinylbenzene

Nobuyuki Tanaka, Minami Nagase, Mitsuru Higa*

Graduate School of Science and Engineering, Yamaguchi University, 2-16-1 Tokiwadai, Ube-city, Yamaguchi 755-8611, Japan
Tel. +81836859203; Fax +81836859201; email: mhiga@yamaguchi-u.ac.jp

Received 1 August 2009; accepted 25 November 2009

ABSTRACT

Organic fouling behavior of anion exchange membranes was examined in an electrodialysis system consisting of commercially available anion exchange membranes, AMX, ASM and ASM-F and NaCl solutions containing sodium dodecylbenzene-sulfonate (DBS) solution as an organic foulant. ASM-F has the highest anti-organic fouling property in all the membranes because of its loose network structure and thin charged layers on the membrane surfaces with the same in sign as the charged group of DBS. The slope of the time–voltage curves through ASM decreases with increasing temperature. This means the organic fouling was suppressed when temperature increase. The permeability coefficient of DBS through the membrane increases with increasing temperature because of the increase in the water content of the membrane. ASM-F has lower permeability coefficient of DBS than ASM at all the temperatures. This means that ASM-F has higher barrier property against DBS than ASM.

Keywords: Organic fouling; Anion exchange membrane; Temperature dependent; Permeability coefficient

1. Introduction

In Japan, hydrocarbon type ion exchange membranes have developed to produce sodium chloride by electrodialytic concentration of seawater. Ion exchange membranes have been applied to many industrial fields such as water treatment [1], food industry [2–4], medical supplies, acid recovery from pickling solution [5–8] and wastewater treatment [9–12] etc. (Fig. 1). To apply the membranes to these industrial fields, organic fouling of ion exchange membranes is one of the major problems in electrodialysis process. Organic fouling of an ion exchange membrane will occur during electrodialysis process using electrolyte solutions containing organic substances. Fig. 2 shows structure of a commercially available anion exchange membrane and a mechanism of organic fouling on the surfaces.

There have been many reports on ion exchange membranes with anti-organic fouling properties. For example, an ion exchange membrane with loosen structure was prepared [13,14]. However, the loosen structure gave the membrane low ionic selectivity and consequently no efficient desalination can be conducted. The introduction of a cation exchange site, sulfonic acid group, onto the surfaces of an anion exchange membrane was investigated [15,16]. However electric resistance was extremely high because of the thick cation exchange layers. Anion exchange group of anion exchange membrane was oxidized at selected chemical sites [17]. Composite membrane prepared from anion exchange membranes and pyrrole is also effective in

---

*Corresponding author

Presented at the Fifth Conference of the Aseanian Membrane Society Aseania 2009 "Recent Progress in Membrane Science and Technology", 12–14 July 2009, Kobe, Japan.

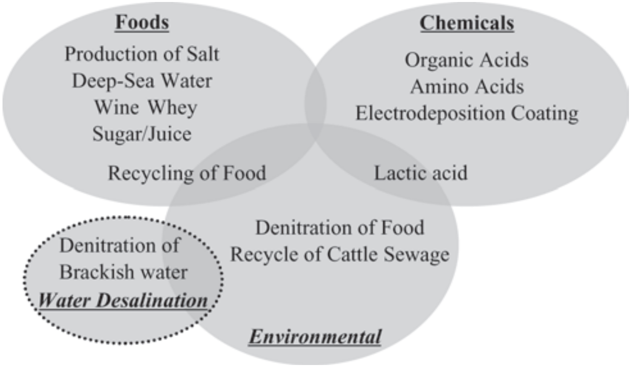

Fig. 1. Applications of electrodialysis process with a hydrocarbon type ion exchange membrane.

preventing the increase in electrical resistance of the membrane and the decrease in current efficiency in the presence of anionic surface active agents [18,19]. However, these two methods also increase the electric resistance of the membranes.

Apart from the pore size and charge effect of an ion exchange membrane, it is thought that one reason for organic fouling of the membranes is based on π–π interaction between the membranes and foulant ions such as aromatic compounds because almost all of ion exchange membranes are prepared from derivatives of styrene-divinylbenzene copolymers; therefore, aliphatic ion exchange membranes have been prepared [20]. However, there are few ion exchange membranes or electrodialysis methods that completely prevent fouling of the membrane by a variety of foulant.

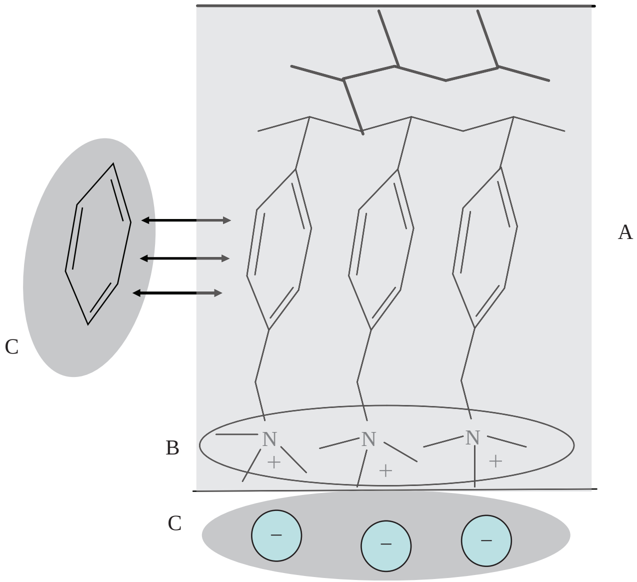

Fig. 2. Suggested mechanism of organic fouling. A, anion exchange membrane; B, anion exchange group of the membrane; and C, organic anion.

Recently, an anion exchange membrane with anti-organic fouling properties was developed, and is sold as Neosepta ASM-F [3]. The membrane has electric charge layer opposite to its fixed charges on its surfaces.

The aim of this study is to investigate fouling mechanism on the surfaces of commercially available anion exchange membranes. Hence, time–voltage curves in an electrodialysis system consisting of an anion exchange membrane and NaCl aqueous solutions containing sodium dodecylbenzene- sulfonate (DBS) as a surface-active agent were measured. Permeation of DBS through the anion exchange membrane during the electrodialysis was also measured.

2. Experimental

2.1. Sample membranes

Commercially available anion exchange membranes [Neosepta AMX, ASM, ASM-F: manufactured by ASTOM Corp.] prepared from chloromethyl styrene and divinylbenzene were used as the sample membrane. Neosepta AMX is the standard grade membrane. Neosepta ASM is a specific grade membrane and has high water contents. Neosepta ASM-F has oppositely electric-charged layers on its surface to prevent organic fouling.

2.1.1. Ion exchange capacity

The membranes were immersed in 0.5 mol dm^{-3} HCl solution during 24 h. Then, they were rinsed with deionized water to remove the non-exchange HCl electrolyte adsorbed in the membranes and immersed in 200 ml of 0.2 mol dm^{-3} $NaNO_3$ under stirring for 12 h in order to obtain the complete exchange of Cl^- ions in the membrane for NO_3^- ions from the solution. The amount of Cl^- ions obtained in the solution was determined by using precipitation titration [21]. Ion exchange capacity C_{ex} of the membranes was calculated from the chloride amount A and the weight of the dry membrane W_b as.

$$C_{ex} = \frac{A}{W_b}. \tag{1}$$

2.1.2. Water content

The membranes were left to soak during 24 h at 25°C in NaCl solutions at different concentrations. The

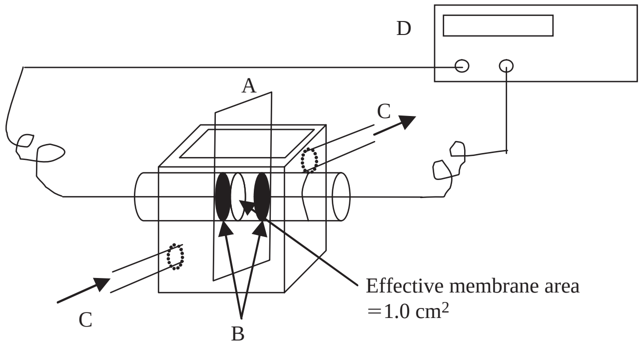

Fig. 3. Apparatus for membrane resistance. A, sample membrane; B, Pt black electrodes; C, NaCl solution; and D, LCR meter. The effective area of the cell is 1.0 cm^2.

membranes were removed from the water, dabbed with filter paper to remove excess water on the membrane surfaces, and wet weight W_a was measured. Dry weight W_b was obtained by drying the samples at 60°C for 24 h. The water content was defined as follows:

$$W = \left(\frac{W_a - W_b}{W_b}\right). \tag{2}$$

2.1.3. Burst strength

Burst strength of ion exchange membrane is expressed by Mullen bursting strength (BS). BS was measured in the wet state with Mullen Burst Tester EL type (Toyo Seiki Seisakusho).

2.1.4. Membrane resistance

''Membrane resistance'' is defined as the division of the electric resistance, measured in 0.5 mol dm^{-3} NaCl solution, by the effective area in this study. Fig. 3 shows an apparatus for electric resistance measurement. A sample membrane was immersed in 0.5 mol dm^{-3} NaCl solution over 2 h. After the membrane was placed between platinum black electrodes, the electric resistance was measured by 1 kHz AC (Hioki 3511-50) at 25.0°C ± 0.2°C (r_1). After the membrane was removed, blank value was measured (r_0). The difference between r_1 and r_0 gives the membrane resistance, R_m.

$$R_m = r_1 - r_0. \tag{3}$$

2.1.5. Membrane thickness

The thickness of the membrane was measured in the wet state with a micrometer (Mitsutoyo MDC-25MJ).

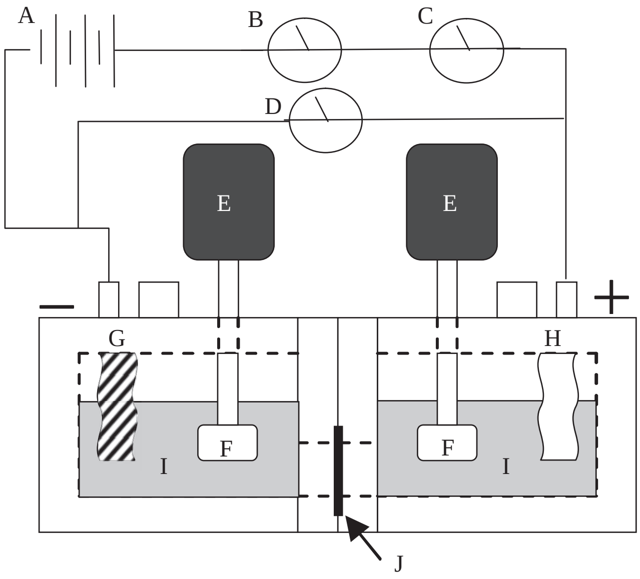

Fig. 4. Apparatus for measuring transport number. A, power supply; B, ampere meter; C, coulomb meter; D, voltmeter; E, motor; F, stirrer; G, cathode electrode; H, anode electrode; I, 0.5 mol dm^{-3} NaCl solution; and J, sample membrane. The effective area of the cell is 8.0 cm^2.

2.1.6. Transport number

To determine the transport number of the membrane, electrodialysis was carried out by using an acrylic plastic cell of two parts separated by a membrane, as shown in Fig. 4 at a current density of 0.01 A cm^{-1} at 25°C for 75 min. The amount of transported ions passed through the membrane during the electrodialysis was measured with using a conductivity meter (HORIBA 3552-10D). The dynamic transport number was obtained in terms of the following equation:

$$t_- = 1.00 - \Delta mF/Q, \tag{4}$$

where t_-, transport number; Δm, amount of transported ions passed through the membrane (mol); Q, amount of electricity passed through the membrane (C); F, Faraday constant (C mol^{-1}). All the experiments were performed at a room temperature.

2.2. Voltage change during electrodialysis period

After soaking in 0.1 mol dm^{-3} NaCl aqueous solution for 1 h and washing with deionized water, a sample membrane was fixed in a 2-compartment cell equipped with a silver electrode and silver chloride electrode (Fig. 5). The anode chamber was filled with 0.1 dm^3 of 0.1 mol dm^{-3} NaCl aqueous solution and the cathode chamber was filled with 0.1 dm^3 of a mixed

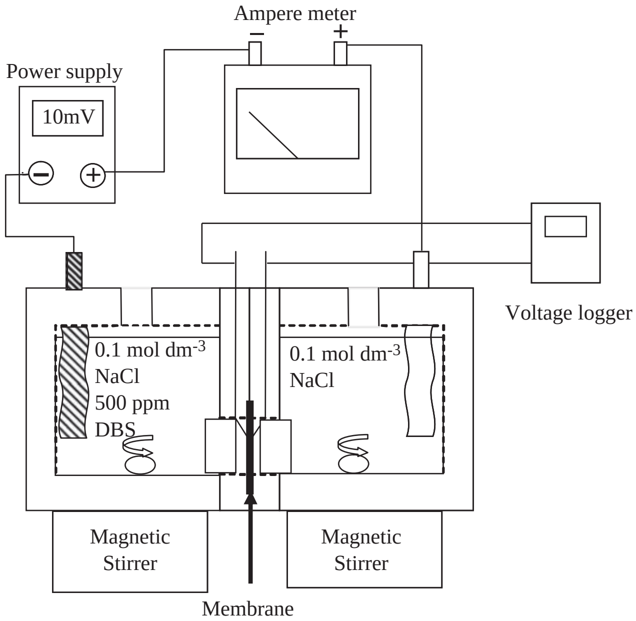

Fig. 5. Apparatus for electrodialysis experiment. One chamber of the cell was filled with a solution of 0.1 mol dm^{-3} NaCl and the other was filled with a mixed solution of 0.1 mol dm^{-3} NaCl and 500 ppm DBS. The current density was 10 mA cm^{-2}. The effective area of the cell is 4.0 cm^2.

solution of 0.1 mol dm^{-3} NaCl and 500 ppm of DBS as a high-molecular-weight organic anion. The solutions in both chambers were stirred at a rotation speed of 1,000 rpm and the electrodialysis was conducted at a current density of 10 mA cm^{-2}. The voltage between the membrane surfaces platinum wire electrodes fixed near the membrane surfaces was measured during electrodialysis period. The voltage between the probe electrodes increases when the organic fouling occurs during the electrodialysis.

2.3. *Permeability coefficient of organic foulant*

After the electrodialysis, the concentration of DBS in the anode chamber was determined with a spectrophotometer for ultraviolet and visible region (Shimazu UV-1600). Permeability coefficient of organic foulant for each membrane was obtained from the concentration change of DBS with electrodialysis time. The permeability coefficient was obtained in terms of the following equation:

$$P = \Delta C V d / \Delta C_0 t S, \tag{5}$$

where P, permeability coefficient of the DBS ($m^2\ s^{-1}$); ΔC, concentration of transported DBS passed through the membrane (ppm); V, volume in the anode chamber (dm^3); d, membrane thickness (mm); ΔC_0, initial concentration of DBS (500 ppm); t, measuring time (s); S, effective area of the cell (=4.0 cm^2).

3. Results and discussion

3.1. *Fundamental properties of anion exchange membranes*

Table 1 shows the fundamental properties of the anion exchange membranes, AMX, ASM, and ASM-F. The membrane resistance of ASM-F is the same as that of ASM although an opposite electric charged layer on membrane surfaces usually gives remarkable increase in the membrane resistance. The membrane resistance as well as other properties of the modified membrane, ASM-F is almost similar to those of the unmodified membrane, ASM. This will be due to the fact that the thickness of the opposite electric charge layers is sufficiently thin.

3.2. *Dependence of membrane structure on organic fouling*

Fig. 6 shows electric potential between the probe electrodes, $\Delta\phi$, as a function of measuring time, t. The electric potential of ASM-F did not change with time while that of the other membranes increases with time. This means that ASM-F has the highest anti-organic fouling property in all the membranes because of its loose network structure and the thin surface charged layers with the same in sign as the charged group of DBS. ASM is better anti-fouling properties than AMX because the water content of ASM is higher than that of AMX.

3.3. *Dependence of temperature on organic fouling*

Figs. 7–9 show electric potential between the probe electrodes, $\Delta\phi$, through AMX, ASM, and ASM-F, respectively, as a function of measuring time operated at 20°C, 25°C, 30°C, and 40°C. The slope of the time–voltage curves of all the membranes decreases with increasing temperature. This means that the organic fouling decreased with increasing temperature. There will be two factors on the decrease in the organic fouling: the decrease in membrane resistance due to the increase in electric conductivity in the membrane; the increase in permeability coefficient of DBS because of the increase in the water content of the membranes [22].

3.4. *Permeability of the organic foulant at various temperatures*

To investigate permeability of the organic foulant at various temperatures, we measured permeability

Table 1
Fundamental properties on commercially available anion exchange membranes. C_{ex} : ion exchange capacity, W : water content, BS : burst strength, R_m : membrane resistance, d : membrane thickness, t_- : transport number

	C_{ex} [mmol g^{-1}]	W [%]	BS [MPa]	R_m [Ω cm^2]	d [mm]	t_- [–]
ASM	1.4	24	0.30	2.3	0.14	0.98
ASM-F	2.0	38	0.32	1.4	0.17	0.98
AMX	2.0	38	0.31	1.4	0.17	0.98

coefficient of fourant through ASM and ASM-F. It was too difficult for AMX to measure the permeability coefficient because of the rapid increase in the voltage by the fouling. Fig. 10 shows the permeability coefficient of DBS as a function of temperature. The permeability coefficient of DBS through both the membranes increases with increasing temperature because of the increasing in the water content. ASM-F has lower permeability coefficient than ASM at all the temperatures. This will be due to the fact that the thin charged layers of ASM-F suppress the permeation of DBS.

4. Conclusions

The electrodialysis under various conditions was carried out to investigate fouling mechanism on the surfaces of the commercially available anion exchange membranes. The lowest voltage change through ASM-F during the electrodialysis period indicates that ASM-F has the highest anti-organic fouling property in all the membranes. This is because its loose network structure and the thin surface charged layers with the same in sign as the charged group of DBS.

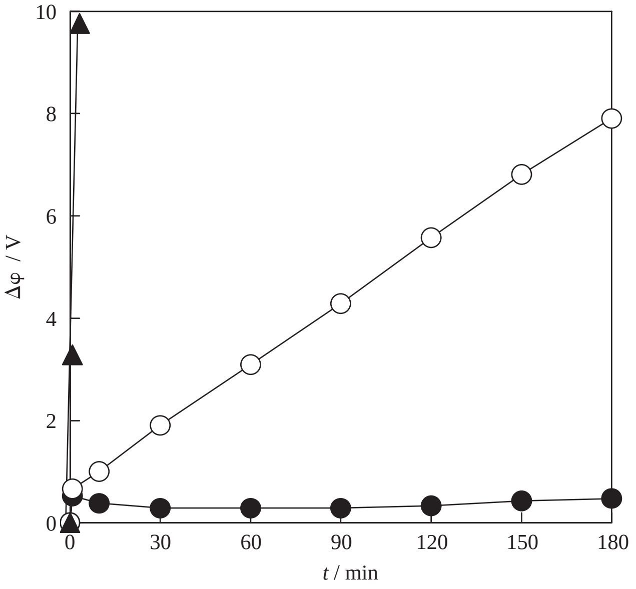

Fig. 6. Electric potential between the probe electrodes, Δϕ, as a function of measuring time, t. Samples: ▲, AMX; ○, ASM; and ●, ASM-F.

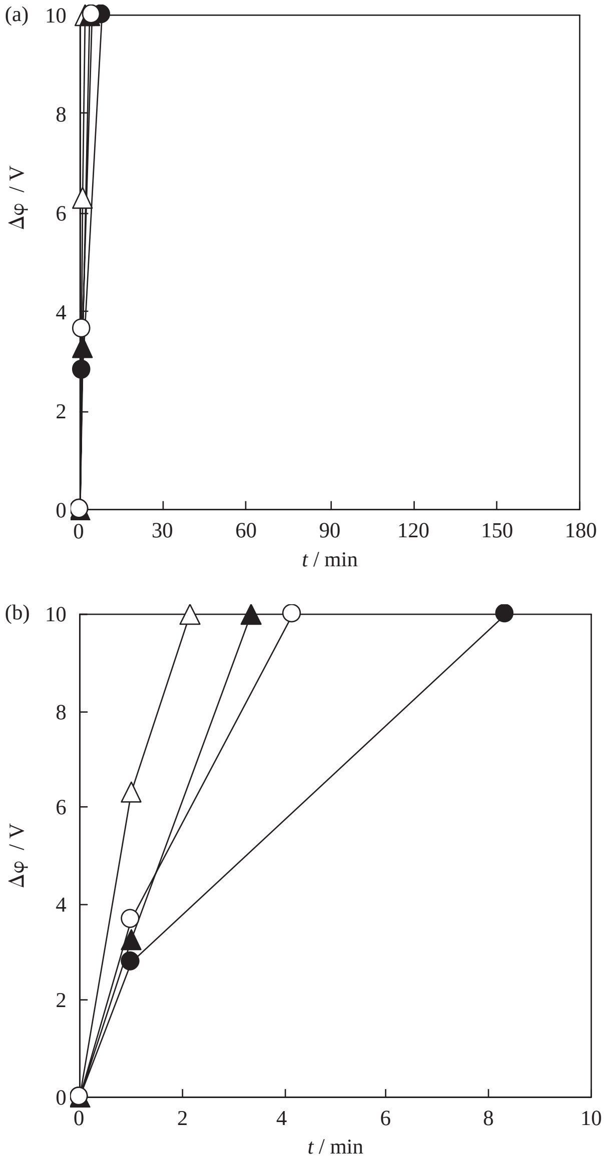

Fig. 7. Electric potential between the probe electrodes, Δϕ, as a function of measuring time, t, of the AMX: (a) total electric potential and (b) initial electric potential. Measuring temperatures: △, 20°C; ▲, 25°C; ○, 30°C; and ●, 40°C.

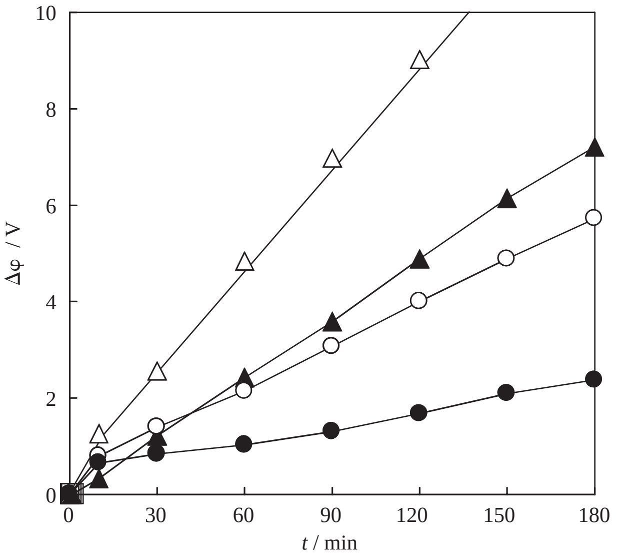

Fig. 8. Electric potential between the probe electrodes, Δϕ, as a function of measuring time, *t*, of the ASM. Measuring temperatures: △, 20°C; ▲, 25°C; ○, 30°C; and ●, 40°C.

The slope of the time–voltage curves through all the membranes decreased with increasing temperature. This means that the organic fouling is suppressed when temperature increase.

The permeability coefficient of DBS through all the membranes increases with increasing temperature because of the increase in the water content. ASM-F has lower permeability coefficient of DBS than ASM at all the temperatures. This means that ASM-F has higher barrier property against DBS than ASM because the thin surface charged layers of ASM-F suppress the permeation of the fourant ions.

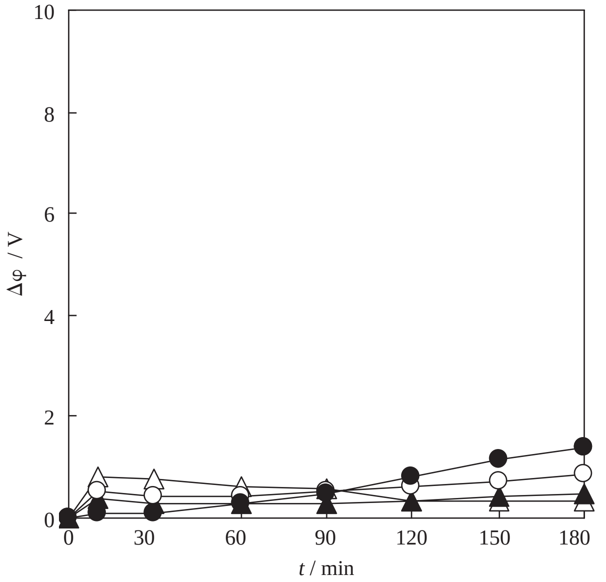

Fig. 9. Electric potential between the probe electrodes, Δϕ, as a function of measuring time, *t*, of the ASM-F. Measuring temperatures: △, 20°C; ▲, 25°C; ○, 30°C; and ●, 40°C.

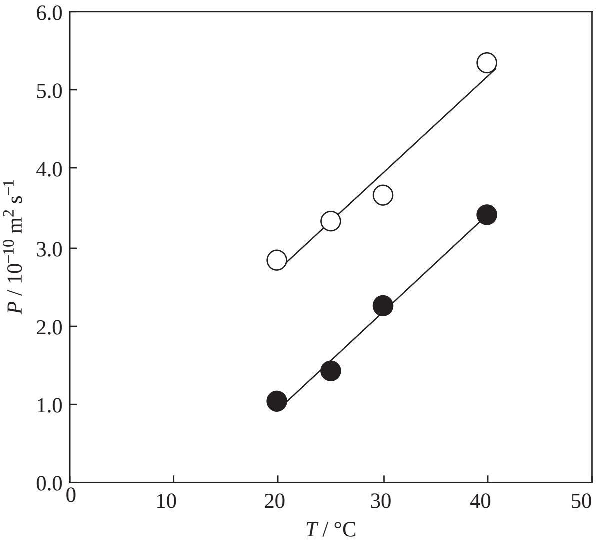

Fig. 10. Permeability coefficient of DBS, *P*, as a function of measuring temperatures, *T*. Samples: ○, ASM and ●, ASM-F.

Acknowledgement

Commercially available anion exchange membranes and some measuring instruments were supplied by ASTOM Corp. This works was partly supported by Electric Technology Research Foundation of Chugoku, the Mazda Foundation, the UBE Foundation, Kurita Water and Environmental Foundation (No. 20320), and the Salt Science Research Foundation, No. 0612, No. 0709 and No. 0810.

Symbols

A	Amount of chloride
W_b	Weight in dry state, g
C_{ex}	Ion exchange capacity, mmol g^{-1} dry membrane: $C_{ex} = A / W_b$
W_a	Weight in wet state, g
W	Water content, g H2O g-1 dry membrane: $W = (W_a - W_b)/W_b$
BS	Burst strength, MPa
r_1	Measured resistance with a sample membrane, Ω cm^2
r_2	Measured resistance without a sample membrane, Ω cm^2
R_m	Membrane resistance, Ω cm^2: $R_m = r_1 - r_2$
d	Membrane thickness, mm
$t-$	Transport number

Δm	Amount of transported ions passed through the membrane, mol
Q	Amount of electricity, C
F	Faraday constant, C mol^{-1}
t	Measuring time, min. or s
P	Permeability coefficient of the DBS, m^2s^{-1}
ΔC	Concentration of transported DBS passed through the membrane, ppm
V	Volume in the anode chamber, dm^3
ΔC_0	Initial concentration of DBS, ppm
ΔS	Effective area of the cell, cm^2
T	Measuring temperature, °C

Greek symbols

$\Delta\phi$	electric potential between the probe electrodes

References

[1] K. Yoshie, MRC News, 36 (2006) 33–35.
[2] M. Iwahara, C. Taniguchi and E. Asada, Japan Patent, JP 4284452 (2009).
[3] N. Tanaka, MRC News, 40 (2008) 72–73.
[4] N. Tanaka, K. Yoshie, T. Aritomi, N. Kanayama and H. Kanayama, Japan Patent, JP 2008-295330 (2008).
[5] Y. Kuboi, Hyomengijyutsu, 50, 8 (1999) 678–682.
[6] A. Pujadas, Pint. Acabados Ind., 38, 230 (1996) 25–31.
[7] U.B. Ogutveren, S. Koparal and E. Ozel, J. Environ. Sci. Eng. Toxic Hazard. Subst. Control, A32, 3 (1997) 749–761.
[8] R. Takeshita, M. Niimoto, T. Aritomi and T. Kobayashi, Japan Patent, JP 2009-39672 (2009).
[9] K. Steenivasarao, F. Patsiogiannis and J. N. Hryn, Light Met. (Warrendale Pa.) (1997) 1153–1158.
[10] Y. Akai, K. Fujii, and S. Seki, Japan Patent, JP H09-271781 (1997).
[11] C. Ueno and M. Sagara, Japan Patent, JP H09-262588 (1997).
[12] Y. Hirose, Japan Patent, JP H08-299962 (1996).
[13] R.B. Hodgdon, E. Witt and S.S. Alexander, Desalination, 13 (1973) 105–127.
[14] K. Kusumoto, H. Ihara and Y. Mizutani, J. Appl. Polym. Sci. 20 (1976) 3207–3213.
[15] K. Kusumoto, T. Sata and Y. Mizutani, 4th International Symposium on Fresh Water from the Sea, Vol. 3 (1973) 111–118.
[16] K. Kusumoto and Y. Mizutani, Desalination, 17 (1975) 111–120.
[17] K. Kusumoto, Y. Mizumoto and Y. Mizutani, Desalination, 17 (1975) 303–311.
[18] T. Sata, J. Chem. Soc., Chem. Commun., 14 (1993) 1122–1124.
[19] T. Sata, J. Phys. Chem., 97 (1993) 6920–6923.
[20] D. Elyanow, R.G. Parent and J.R. Mahoney, Desalination, 38 (1981) 549–565.
[21] T. Sata, ''Ion Exchange Membrane'', The Royal Society of Chemistry, 2004, Chap. 4.2, pp.89–117.
[22] K. Hirayama, F. Hanada, T. Sata and Y. Mizutani, Seventh Symposium on Salt, Vol. II, 1993, 53–58.